Diffractive process in six-prong proton-proton interactions at 205 GeV/c*

M. Derrick, B. Musgrave, P. Schreiner, P. F. Schultz, M. Szczekowski,† and H. Yuta‡
Argonne National Laboratory, Argonne, Illinois 60439
(Received 8 July 1977)

We have studied the 6-prong events in a 50000-picture exposure of the Fermilab 30-inch hydrogen bubble chamber to a 205-GeV/c proton beam. The data consist of complete measurements of 442 events, each containing a proton track with $P_{lab} < 1.4$ GeV/c. A low-mass diffractive peak is seen in the events with 5 charged particles in the forward center-of-mass hemisphere. An analysis based on the rapidity distributions of the outgoing tracks and the missing mass gives a single diffractive cross section of 0.88 ± 0.12 mb for both hemispheres of which the final state $pp\pi^+\pi^+\pi^-\pi^-$ contributes 0.18 ± 0.07 mb. In the diffractive sample, only 0.20 ± 0.06 mb corresponds to events decaying through an intermediate state containing a Δ^{++}. We measure an upper limit for the double diffraction cross section of 0.38 ± 0.12 mb.

Studies of the inclusive proton reaction

$$p + p \to p + X \qquad (1)$$

have been made over a wide range of energies.[1] The data show a low-mass peak in the mass-squared distribution for X (MM^2). In our experiment at 205 GeV/c in the 30-inch hydrogen bubble chamber at the Fermi National Accelerator Laboratory, it was found that only the low-multiplicity events (two, four, and six prongs) contribute[2] to this diffractive enhancement. Detailed studies of the two- and four-prong events show that their single diffractive contributions to the low-mass peak are 2.05 ± 0.22 mb and 2.38 ± 0.16 mb, respectively.[3,4] In the four-prong events, 25% of the low-mass peak was found to come from the $pp\pi^+\pi^-$ final state, with the remainder consisting of states with three or more pions. From an analysis of the missing-mass spectrum, the six-prong events were estimated to contribute 0.52 ± 0.18 mb to the total diffractive cross section.[2] All these numbers are quoted for both center-of-mass (c.m.) hemispheres.

In this paper we report on our study of the complete six-prong events and on their contribution to the low-mass peak observed in reaction (1). Previously,[2] only the slow proton was measured and no information was obtained about the individual make-up of the system X. The new results come from measurements of all outgoing tracks for those six-prong events, in a given fiducial region, which had a proton with laboratory momentum less than 1.4 GeV/c. Our selected data sample consists of 442 events corresponding to a μb equivalent of 6.06 μb/event.

We first present the evidence for diffractive dissociation of the beam particle. Figure 1(a) shows the square of the missing mass, MM^2, of the system recoiling from the slow proton. In Figs. 1(b)–1(f) we show this MM^2 distribution subdivided ac-

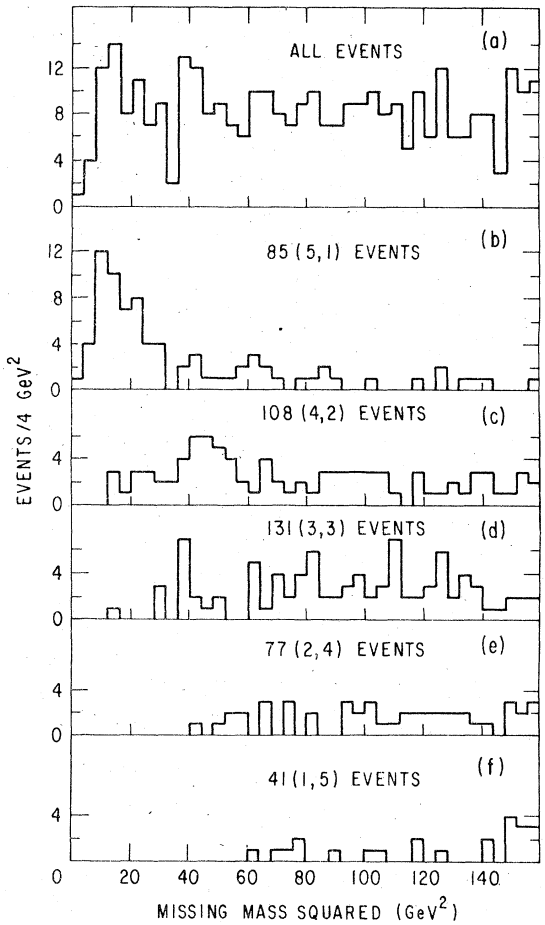

FIG. 1. Missing-mass-squared (MM^2) distributions for the system recoiling from the slow proton in six-prong events: (a) all events, (b) 85 events with five particles in the forward c.m. hemisphere, (c) 108 events with four particles in the forward c.m. hemisphere, (d) 131 events with three particles in the forward c.m. hemisphere, (e) 77 events with two particles in the forward c.m. hemisphere, and (f) 41 events with one particle in the forward c.m. hemisphere.

cording to the number of charged particles in the forward c.m. hemisphere. We refer to events with i charged particles in the forward c.m. hemisphere and j charged particles in the backward c.m. hemisphere as (i,j) events. We note that the events with low MM^2 are almost all of the (5, 1) type, with a small contribution from the (4, 2) events.

To continue the analysis, we consider the particle distributions in the ordered rapidity chain. We use the pseudorapidity variable

$$\eta = \ln \tan \tfrac{1}{2}\theta , \tag{2}$$

where θ is the laboratory production angle for an outgoing particle. For those events in which the beam particle diffractively dissociates, we expect the recoiling target proton to be well separated from the remaining particles in the ordered rapidity chain as shown in Fig. 2.

In our study of the diffractive process in the four-prong events, we used the technique of rapidity-gap analysis and a minimum rapidity gap $\Delta\eta = 2.5$ was found appropriate to define diffraction. Figure 3(a) shows the MM^2 distribution for the six-prong events which have a proton on the left-hand end of the rapidity chain in Fig. 2, and for which the largest η gap is also the first gap. Comparing this to Fig. 1(a), we note that almost all the events with $MM^2 < 40$ GeV^2 appear in Fig. 3. The cross-hatched events have the first gap greater than 2.5 units. For these events, the average η of the five particles is 4.6 units and the average spread in η for the five-particle cluster is 2.3 units. Using the same definition as was previously used for the four-prong events, we find 64 events with $\Delta\eta > 2.5$ units and $MM^2 < 40$ GeV^2. This corresponds to a single diffractive cross section of 0.88 ± 0.12 mb,[5] which is somewhat larger than the diffractive cross section of 0.52 ± 0.18 mb estimated from an analysis of the MM^2 distribution only.[2] Our definition of diffraction involves no background subtraction and does allow some pions to be in the backward hemisphere.

To estimate the contribution to the diffractive peak from the reaction

$$pp \to pp\pi^+\pi^+\pi^-\pi^- , \tag{3}$$

we have fitted the six-prong events with the kinematic fitting program SQUAW and looked for three- or four-constraint fits. Since we are interested in fits for which a proton is the fastest particle in the lab frame, we accepted only those fits for which the fast forward proton had laboratory momentum > 150 GeV/c. Our previous analyses[3,4] of the inclusive distribution in Feynman x ($x = P_{\parallel}/2\sqrt{s}$) for positive pions show very few events with $|x| > 0.6$, and so we have also required the π^+ laboratory momentum to be < 110 GeV/c (corresponding to $x < 0.6$). In Fig. 3(b) we show the distribution in MM^2 from the slow proton for the events with accepted fits to reaction (3), and for which the largest η gap is the first gap. Almost all events have $MM^2 < 20$

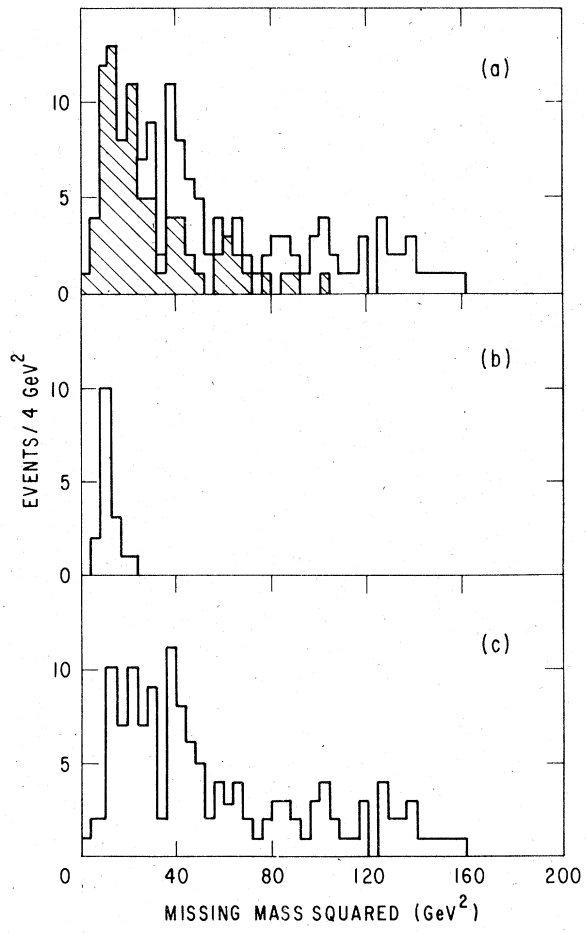

FIG. 3. Missing-mass-squared (MM^2) distribution for the system recoiling off the slow proton for those events with the proton on the end of the ordered rapidity chain and for which the largest rapidity gap is the one separating the proton from its nearest neighbor: (a) all six-prong events, (b) events giving acceptable fits to the reaction $pp \to pp\pi^+\pi^+\pi^-\pi^-$, (c) remaining events, i.e., the difference between (a) and (b). The cross-hatched events correspond to those for which the first gap is greater than 2.5 units.

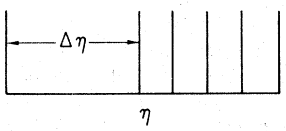

FIG. 2. Configuration of particles in $\eta = \ln \tan \frac{1}{2}\theta$ for a beam diffraction dissociation in a six-prong event.

TABLE I. Properties of the low-mass diffractive enhancement in $pp \to pX$ at 205 GeV/c.

	Composition of final state	Approximate MM^2 peak position (GeV^2)	Cross section (mb) (both hemispheres)
2-prong inelastic	$N+\geq 1\pi$	2	2.04 ± 0.22
4-prong events			
3C-4C fits	$p\pi^+\pi^-$	4.5	0.64 ± 0.14
remaining 4-prong events	$N+\geq 3\pi$	10	1.92 ± 0.16
6-prong events			
3C-4C fits	$p\pi^+\pi^+\pi^-\pi^-$	10	0.18 ± 0.07
remaining 6-prong events	$N+\geq 5\pi$	20	0.70 ± 0.11

GeV^2 and correspond to a cross section of 0.18 ± 0.07 mb, 20% of the total six-prong diffractive cross section.[6]

Figure 3(c) shows those diffractive events which do not have accepted fits to reaction (3). Note that the peak is at a higher value of MM^2 than for the events assigned to reaction (3). This agrees with earlier observations that the diffractive peak moves up in MM^2 as the number of constituent particles increases.[4] The results for the various topologies are compared in Table I and illustrated in Fig. 4, which shows the diffractive peak for various topologies, both with and without missing neutrals.

In a companion study,[7] we have determined the characteristics of inclusive Δ^{++} production. One interesting question is the extent to which the Δ^{++} results from the decay of a higher-mass diffractively-produced state. Since the Δ^{++} inclusive cross section is about equal to the diffractive cross section for the six-prong events, this topology is important for a study of the connection between diffraction and Δ^{++} production. To investigate this question, we have chosen the events that are symmetric in the c.m. system to the (5, 1) events of Fig. 1(b). In Fig. 1 we see that there are only 41 (1, 5) events present, whereas we observe 85 (5, 1) events. After making a 15% correction for events with two fast protons[5] ($P_{lab} > 1.4$ GeV/c), this implies that about 35% of the (5, 1) events contain a neutron in the final state.

Figure 5(a) shows the $p\pi^+$ mass distribution for the (1, 5) in which the target has diffracted. A clear peak corresponding to Δ^{++} production is observed. This peak of 18 events above background gives a cross section of 0.22 ± 0.06 mb, which may be compared to the inclusive six-prong Δ^{++} cross section of 0.80 ± 0.10 mb.[7] Thus there is only about a 25% overlap between diffraction and Δ^{++} production for the six-prong topology. In Fig. 5(b) the diffractive events also show an enhancement in the Δ^0 region, but the small number of events and the uncertainty in the background do not allow us to make a quantitative estimate of the Δ^0 cross section.

We have also studied double diffraction dissociation $pp \to N^*N^*$, where the symbol N^* is used here

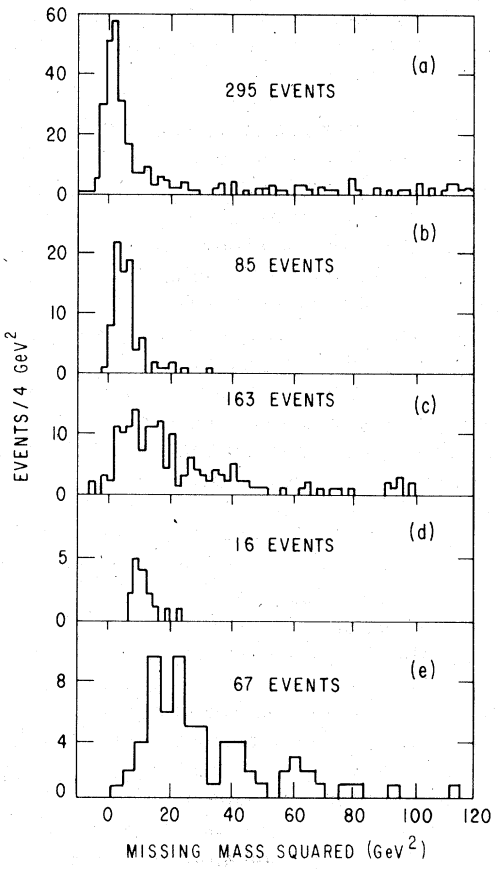

FIG. 4. Missing-mass-squared (MM^2) distribution for the system recoiling from the slow proton for (a) the inelastic two-prong events, (b) the (3,1) four-prong events fitting $pp \to pp\pi^+\pi^-$, (c) the remaining four-prong events, (d) the (5,1) six-prong events fitting $pp \to pp\pi^+\pi^+\pi^-\pi^-$, (e) remaining six-prong events.

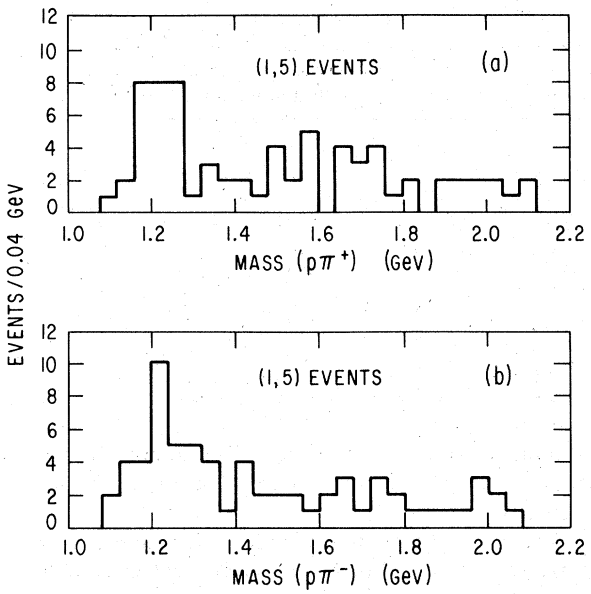

FIG. 5. (a) Effective mass of slow proton plus π^+ for the (1,5) events; there are two entries per event. A Δ^{++} signal is evident. (b) Effective mass of slow proton plus π^- for the (1,5) events.

to refer to the low-mass enhancement which decays into three charged particles (with or without neutrals). The signal for this reaction is shown in Fig. 6 as a correlated low-mass enhancement, both in the mass of slow proton, positive and negative pion system, and in the missing mass to this system. From the six combinations that are candidates for $p\pi^+\pi^-$, we have selected one per event. To be selected, the combination must have mass squared less than 40 GeV^2 and momentum transfer from the target proton lower than in any other such combination. To estimate the background, we have repeated the same selection procedure for the non-diffractive combinations $p\pi^-\pi^-$. The $p\pi^+\pi^-$ and $p\pi^-\pi^-$ mass distributions are shown in Fig. 7(a) as the open and cross-hatched histograms, respectively. There is a clear excess of the signal ($p\pi^+\pi^-$) over the background ($p\pi^-\pi^-$). Figure 7(b) shows the MM^2 distribution from the events of Fig. 7(a) where now the open histogram corresponds to the missing mass recoiling off the $p\pi^+\pi^-$ system of Fig. 7(a) and the cross-hatched histogram to that recoiling of the $p\pi^-\pi^-$ system. Since we are interested in the shape of the background to the MM^2 distribution, we have area-renormalized the cross-hatched histogram to the open histogram in Fig. 7(b). Although there is an excess at low MM^2 in Fig. 7(b), the large backgrounds and unknown correlations between the signal and background in Figs. 7(a) and 7(b) only allow us to establish an upper limit for double diffraction. From Fig. 7(b), we obtained $\sigma_{DD} \leq 0.38 \pm 0.12$ mb.[8]

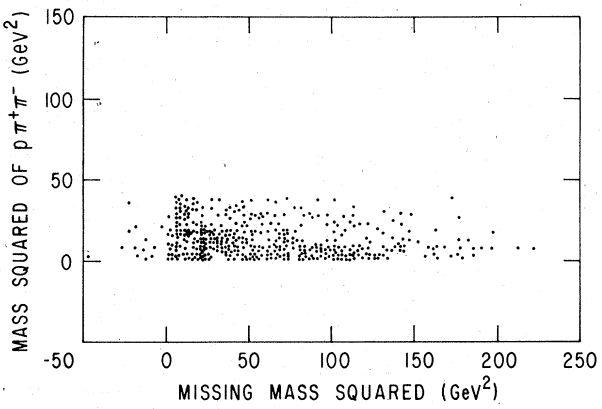

FIG. 6. Scatter plot of $M^2(p\pi^+\pi^-)$ vs the missing mass squared. There is one entry per event selected as that $p\pi^+\pi^-$ combination with $M^2(p\pi^+\pi^-) < 40$ GeV^2 and the lowest momentum transfer from the target proton.

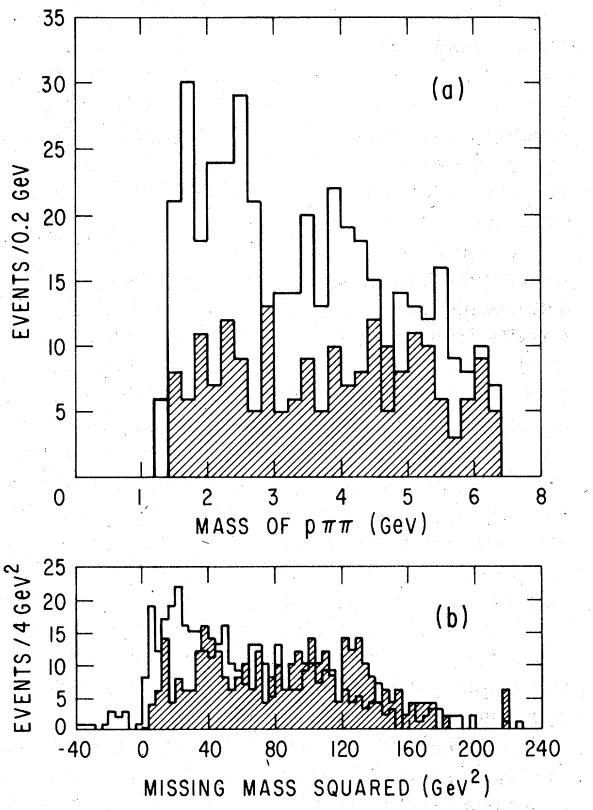

FIG. 7. (a) Distribution in $M(p\pi^+\pi^-)$, one combination per event with $M^2(p\pi^+\pi^-) < 40$ GeV^2, and the combination with lowest momentum transfer chosen. The cross-hatched events represent the background $p\pi^-\pi^-$ combinations. (b) Distribution in the square of the missing mass for the system recoiling against the selected $p\pi^+\pi^-$ system. The cross-hatched events represent the background using the system recoiling against the $p\pi^-\pi^-$ combinations.

*Work supported by the U. S. Energy Research and Development Administration.

†On leave of absence from the Institute for Nuclear Research, Warsaw, Poland.

‡Present address: Tohoku University, Sendai 980, Japan.

[1]See, for example, J. Whitmore, Phys. Rep. 10C, 273 (1974); 27C, 187 (1976).

[2]S. J. Barish *et al.*, Phys. Rev. Lett. 31, 1080 (1973).

[3]S. J. Barish *et al.*, Phys. Rev. D 9, 1171 (1974).

[4]M. Derrick *et al.*, Phys. Rev. D 9, 1215 (1974); 9, 1853 (1974).

[5]A 15% correction results from requiring symmetry in the c.m. system. In the $pp\pi^+\pi^+\pi^-\pi^-$ events, we find 30% fewer slow (target-associated) protons than fast (beam-associated) protons. This is due to the cutoff at a laboratory momentum of 1.4 GeV/c that was applied to select the slow protons. We apply the same 15% correction to all 6-prong events.

[6]Following the analysis described in Ref. 4 for the reaction $pp \to pp\pi^+\pi^-$, we have subtracted a background of $(20 \pm 7)\%$ to account for events which actually have one or more missing neutrals.

[7]S. J. Barish *et al.*, Phys. Rev. D 12, 1260 (1975).

[8]In a study of six-prong events at 300 GeV/c, A. Firestone *et al.*, Phys. Rev. D 12, 15 (1975), report a $\sigma_{DD} = 0.12 \pm 0.05$ mb.